Chaos
An Interdisciplinary Journal of Nonlinear Science

RESEARCH ARTICLE | JULY 10 2025

Explosive synchronization in generalized multiplex network with competitive and cooperative interlayer interactions

Palash Kumar Pal ; Nikita Frolov ; Sarbendu Rakshit ; Alexander E. Hramov ; Dibakar Ghosh

Chaos 35, 071102 (2025)
https://doi.org/10.1063/5.0283789

Articles You May Be Interested In

AIP Publishing

Chaos ARTICLE pubs.aip.org/aip/cha

Explosive synchronization in generalized multiplex network with competitive and cooperative interlayer interactions

Cite as: Chaos 35, 071102 (2025); doi: 10.1063/5.0283789
Submitted: 3 June 2025 · Accepted: 25 June 2025 ·
Published Online: 10 July 2025

Palash Kumar Pal,[1] Nikita Frolov,[2] Sarbendu Rakshit,[3] Alexander E. Hramov,[4] and Dibakar Ghosh[1,a)]

AFFILIATIONS

[1] Physics and Applied Mathematics Unit, Indian Statistical Institute, 203 B. T. Road, Kolkata 700108, India
[2] Laboratory of Dynamics in Biological Systems, Department of Cellular and Molecular Medicine, KU Leuven, Herestraat 49, 3000 Leuven, Belgium
[3] Department of Sciences and Humanities, Indian Institute of Information Technology, Design and Manufacturing Kancheepuram, Chennai 600127, India
[4] Baltic Center for Neurotechnology and Artificial Intelligence, Immanuel Kant Baltic Federal University, 14 A. Nevskogo ul., Kaliningrad 236016, Russia

[a)] **Author to whom correspondence should be addressed:** dibakar@isical.ac.in

ABSTRACT

Explosive synchronization represents an abrupt first-order transition to coherence in coupled dynamical systems, with significant implications for real-world networks such as neural systems, power grids, and social networks. In this study, we investigate explosive synchronization in adaptive multiplex networks of an arbitrary number of layers with the coexistence of competitive and cooperative interlayer interactions, where the dynamics of a node in one layer is influenced by the coherence of its counterparts in other layers. In addition to these interlayer interactions, our model incorporates interlayer adaptive coupling that can be simultaneously cooperative and competitive. Using a generalized framework, we show that the fraction of competitive nodes f_l within each layer critically impacts the synchronization dynamics. Higher fractions suppress synchronization, while lower fractions promote the degree of synchronization transition. As the number of layers increases, the hysteretic behavior associated with explosive synchronization becomes more pronounced, highlighting enhanced resilience in synchronization transitions. The analytical predictions derived from the mean-field approach align closely with the numerical simulations across networks with an arbitrary number of layers, validating the robustness of the proposed framework. This scalability across multiplex networks underscores the critical role of adaptive interdependencies in shaping synchronization patterns. These findings provide a comprehensive understanding of how multiplex architectures govern the dynamics of explosive synchronization and provide insight into controlling synchronization in complex systems.

From the discovery of explosive synchronization in dynamical networks, it was believed that the correlation between the degree of each node, coupling strength, and frequency of the Kuramoto oscillators played a vital role in its emergence. Later, these restrictions were removed by introducing an adaptive network with interdependent and competitive interactions. This work presents an adaptive network where these two adaptive interactions work simultaneously. Due to a fraction of interdependent and competitive interactions, suppressing the formation of giant clusters leads to a hysteresis loop for bistability. Then, we generalize the phenomenon for multiplex networks with the arbitrary number of layers. We analytically verify our results using the mean-field approach.

I. INTRODUCTION

When an ensemble of oscillators interacts, increasing/decreasing the coupling strength, a continuous and smooth transition is observed from an incoherent to a coherent state. This transition type is known as a second-order phase transition.[1,2] In this transition, more oscillators join the coherent group by varying the coupling strength and, finally, become one coherent group. In some cases, the transition from incoherent to coherent occurs suddenly at a critical value of the coupling strength. This type of transition is irreversible and not continuous, commonly known as a first-order phase transition in statistical physics. In nonlinear dynamical systems, the first-order transition is also known as explosive synchronization (ES).[3] Since its investigation[4] in 2005, it has become an exciting field of research due to its diverse significance in different fields, such as cascading collapse in power grid networks,[5] neuronal spiking in the human brain,[6] opinion dynamics in social networks,[7] internet jamming,[8] etc. The ES is observed in complex dynamical systems by introducing a correlation between the local dynamics of the node, the degree of each node, and the coupling strength. From its discovery, it was believed that any correlation was required for the emergence of ES. The ES is characterized by bistability behaviors in the hysteresis between the critical coupling strengths of forward and backward transitions. Later, this ES is also observed in different network topologies, such as multiplex network,[9] introducing time-delay coupling,[10] dynamically dissimilar multiplex networks,[11] interlayer Hebbian plasticity,[12,13] considering higher-order interactions in networks,[14,15] etc.

Recently, it was observed that ES could emerge by introducing an adaptive controller by a local order parameter.[16] The adaptation in the coupling may be cooperative or competitive type, and different synchronization phenomena are observed.[17–19] Using an attractive and repulsive type adaptation, various kinds of ES are observed in dynamic networks.[20,21] The explosive transition from an incoherent to a coherent state is explored in interdependent and competitive interactions in multiplex networks. It discusses the variation of the hysteresis region due to a mixed adaptive mechanism.[22]

In general, the interactions between dynamical systems occur in two different ways, namely, interdependent (cooperation) interactions and competitive (inhibition) interactions.[23–25] In interdependent interactions, one node is influenced by the neighboring nodes and is represented by multiplying the local order parameters with the coupling strength and observed ES state.[16] By increasing the coupling strength, more oscillators join in the coherent group and the system exhibits an abrupt transition from incoherent to coherent states. On the other hand, repulsion between the nodes exists through competitive interactions, which is usually seen between the prey and predator in ecological systems,[26] cooperator–defector in the evolutionary game theory,[27,28] etc. In some natural systems, both the interactions co-occur, for example, simultaneous presence of excitatory and inhibitory synaptic interactions between neurons,[29,30] competitors and cooperators in sociology,[31] and for the modeling of biological[32] and physical[33] systems. Previously, the ES was observed in multiplex networks with non-adaptive excitatory and inhibitory layers.[34] In another study, the ES is observed in an adaptive coupling with a multiplex network configuration using interdependent interactions only.[16] Also, the coexistence of competitive and cooperative interlayer interactions in a two-layer multiplex network has been studied by Frolov *et al.*[22] and Xie *et al.*,[35] but it is assumed that the replica nodes that are interconnected via the adaptive mechanism are of the same type; they are both either cooperative or competitive in the multiplex network model.

In this paper, we aim to address the following central questions: Is it possible to observe ES in a multiplex network of coupled oscillators where the interlayer interactions include not only simultaneous interdependent and competitive couplings but also mixed-mode interactions—where one node exhibits cooperative behavior while its counterpart in the interconnected layer displays competitive behavior? How do these adaptive and heterogeneous interlayer interactions influence the onset and nature of explosive synchronization in such multiplex configurations?

To answer these questions, we consider a multiplex network of an arbitrary number of layers, where the local order parameters of the nodes in each layer control the adaptive mechanism. Here, we choose a fraction f of the nodes in each layer so that we can divide them into two groups, for instance, a competitive group that inhibits the coupling strength and a cooperative group that enhances the coupling strength, and they are adaptively controlled by the local order parameter of the counterpart nodes of the remaining layers in two ways. These fraction values, in general, might not be equal, so by the proposed adaptive mechanism, the counterpart nodes can be of the same type (either they are both cooperative or competitive) or a different type (one cooperative and another competitive). We show that ES emerges, indeed, when the value f is small enough, but when its value is high, we see continuous and reversible phase transitions of the global order parameters of the layers. We also provide the analytical treatments to verify the steady-state behavior of this multiplex network model in the continuum limit.

II. ADAPTIVE MULTIPLEX NETWORKS WITH AN ARBITRARY NUMBER OF LAYERS

To broaden and expand the study of ES in a bilayer multiplex network, which incorporates both interdependence and competition,[22] we examine a multiplex network with an arbitrary number of layers (L), where each layer is characterized by a specific fractional value of competitive units. The dynamics of such a network is governed by the following system of coupled differential equations:

$$\dot{\theta}_{l,i}(t) = \omega_{l,i} + \lambda \mathcal{D}_{l,i}(t) \sum_{j=1}^{N} \mathscr{A}_{ij}^{[l]} \sin(\theta_{l,j} - \theta_{l,i}), \tag{1}$$

where $i = 1, 2, \ldots, N$ indexes the oscillators in each layer, $l = 1, 2, \ldots, L$ denotes the layer index, and $\mathscr{A}_{ij}^{[l]}$ represents the adjacency matrix of the lth layer. If nodes i and j in the lth layer are connected, $\mathscr{A}_{ij}^{[l]} = 1$, and $\mathscr{A}_{ij}^{[l]} = 0$ otherwise. Here, $\omega_{l,i}$ is the natural frequency of the ith oscillator in the lth layer and λ denotes the coupling strength.

The key feature of this framework is the adaptive core $\mathcal{D}_{l,i}(t)$, which determines the type of interaction, whether it is competitive or interdependent between oscillators in the layers. The dynamics of $\mathcal{D}_{l,i}(t)$ is influenced by the coherence of the remaining $(L-1)$ replica nodes of the oscillator i in the other layers. For a fraction f_l of competitive nodes in the layer l, the adaptation function is given by

$$\mathcal{D}_{l,i}(t) = 1 - \frac{1}{L-1} \sum_{l' \neq l} r_{l',i}(t), \tag{2}$$

where $r_{l',i}(t)$ represents the amplitude of the local Kuramoto order parameter of the ith oscillator in the layer l'. It is defined as

$$r_{l',i}(t)e^{\mathrm{i}\phi_{l',i}} = \frac{1}{k_{l',i}}\sum_{j=1}^{N}\mathscr{A}_{ij}^{[l']}e^{\mathrm{i}\theta_{l',j}(t)}, \quad \mathrm{i}=\sqrt{-1}, \tag{3}$$

where $k_{l',i} = \sum_{j=1}^{N}\mathscr{A}_{ij}^{[l']}$ is the degree of the ith oscillator in the layer l'. This formulation ensures that competitive nodes are negatively influenced by the coherence in the other layers.

For the remaining fraction $(1-f_l)$ of interdependent nodes, the adaptation function aligns positively with the coherence in the other layers as

$$\mathcal{D}_{l,i}(t) = \frac{1}{L-1}\sum_{l'\neq l} r_{l',i}(t). \tag{4}$$

This adaptive mechanism allows for the coexistence of distinct populations in the multiplex network, where some nodes exhibit competitive behavior while others are interdependent. The proportion f_l can vary across layers, enabling each layer to exhibit unique synchronization dynamics influenced by the interlayer coherence.

This generalized framework [Eq. (1)] demonstrates that the addition of layers enhances the complexity and robustness of ES, as evidenced by widened hysteresis loops and abrupt first-order synchronization transitions. This model is both scalable and versatile, providing a foundation for understanding synchronization phenomena in real-world multiplexed systems, such as neural networks, power grids, and social networks.

III. THEORETICAL ANALYSIS

In this section, we analytically investigate the dynamics of the proposed multiplex adaptive network model [Eq. (1)], incorporating both competitive and interdependent interactions between the arbitrary number of layers.

For the multiplex network consisting of L layers, governing equation (1) can be expressed in terms of the order parameters as

$$\dot{\theta}_{l,i} = \omega_{l,i} + \lambda\mathcal{D}_{l,i}r_{l,i}k_{l,i}\sin(\phi_{l,i}-\theta_{l,i}). \tag{5}$$

Now, we use the mean-field approximations; in this framework $r_{l,i} = R_l$, $\phi_{l,i} = \Psi_l$, where R_l is the amplitude of the global order parameter of the lth layer and Ψ_l represents the average phase of the oscillators in that layer defined as $R_l e^{\mathrm{i}\Psi_l} = \frac{1}{N}\sum_{j=1}^{N}e^{\mathrm{i}\theta_{l,j}}$. The adaptive core $\mathcal{D}_{l,i}$ is taken as the average of all adaptive terms over competitive and interdependent units of layer l as

$$\mathcal{D}_{l,i} = f_l\left(1-\frac{1}{L-1}\sum_{l'\neq l}r_{l',i}\right) + (1-f_l)\frac{1}{L-1}\sum_{l'\neq l}r_{l',i}. \tag{6}$$

Therefore, if we consider $\Delta\theta_{l,i} = \theta_{l,i}-\Psi_l$ and $\dot{\Psi}_l = \Omega_l$, then Eq. (5) becomes

$$\Delta\dot{\theta}_{l,i} = \omega_{l,i} - \Omega_l - \lambda R_l\mathcal{D}_l' k_{l,i}\sin(\Delta\theta_{l,i}), \tag{7}$$

where $\mathcal{D}_l' = f_l + \frac{1-2f_l}{L-1}\sum_{l'\neq l}R_{l'}$.

The ith oscillator in the layer l reaches a phase-locked state if

$$\Delta\theta_{l,i} = \arcsin\left(\frac{\omega_{l,i}-\Omega_l}{\lambda R_l\mathcal{D}_l' k_{l,i}}\right), \tag{8}$$

with the condition $|\omega_{l,i}-\Omega_l| \le \lambda R_l\mathcal{D}_l' k_{l,i}$. Otherwise, the oscillators drift indefinitely.

If the natural frequency distribution $g(\omega_{l,i})$ is symmetric, the average frequency Ω_l becomes identically zero. For phase-locked oscillators, we then have

$$\Delta\theta_{l,i} = \arcsin\left(\frac{\omega_{l,i}}{\lambda R_l\mathcal{D}_l' k_{l,i}}\right), \tag{9}$$

where $|\omega_{l,i}| \le \lambda R_l\mathcal{D}_l' k_{l,i}$.

The global order parameter R_l for the lth layer can be rewritten as

$$\begin{aligned} R_l\exp(\mathrm{i}\Psi_l) &= \frac{1}{\sum_{j=1}^{N}k_{l,j}}\sum_{j=1}^{N}k_{l,j}r_{l,j}\exp(\mathrm{i}\phi_{l,j}) \\ &= \frac{1}{N\langle K_l\rangle}\sum_{j=1}^{N}k_{l,j}\exp(\mathrm{i}\theta_{l,j}), \end{aligned} \tag{10}$$

where $\langle K_l\rangle = \frac{\sum_{j=1}^{N}k_{l,j}}{N}$ is the average degree of the lth layer. Assuming that the contribution of drifting oscillators to R_l is negligible, the order parameter can be expressed as

$$R_l = \frac{1}{N\langle K_l\rangle}\sum_{|\omega_{l,i}|\le\lambda R_l\mathcal{D}_l' k_{l,i}} k_{l,i}\sqrt{1-\left(\frac{\omega_{l,i}}{\lambda R_l\mathcal{D}_l' k_{l,i}}\right)^2}. \tag{11}$$

For the thermodynamic limit, the summation can be replaced by integration, leading to

$$R_l = \frac{1}{\langle K_l\rangle}\int_{\mathbf{B}_l}P(K_l)g(\omega_l)K_l\sqrt{1-\left(\frac{\omega_l}{\lambda R_l\mathcal{D}_l' K_l}\right)^2}\,d\omega_l\,dK_l, \tag{12}$$

where $P(K_l)$ represents the degree distribution of the intralayer network in the layer l, and $\mathbf{B}_l$ is the region in the (K_l,ω_l) plane defined by $|\omega_l| \le \lambda R_l\mathcal{D}_l' K_l$.

IV. VERIFICATION OF ANALYTICAL FINDINGS

To verify the theoretical results, we first consider a multiplex network of two layers, and then a multiplex network with $L=3$ layers. Numerical simulations are conducted to observe the forward and backward phase transitions of the global order parameters R_1, R_2, and R_3 with respect to the coupling strength λ. The results confirm the analytical predictions, demonstrating the emergence of hysteretic behavior and abrupt synchronization transitions as the fraction f_l of the competitive nodes varies. In the numerical simulations, the network topology in each layer is modeled as a random Erdős–Rényi (ER) network consisting of $N=10^3$ nodes. We have explored various multiplex network configurations by varying the fraction of competitive units in each layer and the average degree of the nodes within those layers. The natural frequencies $\omega_{l,i}$ of the ith oscillator in the lth layer are drawn uniformly from the interval $[-1,1]$, while the initial phases $\theta_{l,i}$ are distributed uniformly within the range $[0, 2\pi)$. However, we have also considered a bilayer network setup in which one layer is a scale-free network with a heterogeneous degree distribution of nodes and has a frequency distribution as the standard Cauchy distribution (see the Appendix). The governing Eq. (1) is integrated numerically using the fourth-order Runge–Kutta (RK4) method. The integration is performed with a fixed time step of $\Delta t = 10^{-2}$ time units, a maximum simulation time of $t_{\max} = 10^5$ iterations, and a transient period of $t_{\mathrm{tr}} = 5 \times 10^4$ iterations.

To solve the system of Eq. (11), which comes from the theoretical analysis, we employ the Newton–Raphson method, a widely used iterative technique for solving nonlinear equations. Specifically, we start with initial guesses for $r_1, r_2, \ldots, r_L$ from the interval $(0, 1)$ and refined these values iteratively. At each iteration, we calculate the Jacobian matrix of the system and update the solution using Newton's update rule until the values converge within a predefined tolerance of 10^{-6}. This numerical approach ensures the accuracy and stable solutions of the order parameters, allowing us to effectively analyze synchronization transitions in the multiplex network.

To investigate the synchronization profiles of each layer, we adiabatically vary the coupling strength λ for different values of fractions f_l of competitive nodes and average degree $\langle K_l \rangle$ of the lth layer. Specifically, λ is increased (or decreased) within the range $[0.0, 0.5]$ with step size $\delta\lambda = 0.01$. We first consider a bilayer multiplex network to validate the analytical calculations in Eq. (11). We consider two types of network configurations, namely,

(1) coexistence of competitive and cooperative nodes in both layers, and each pair of replica nodes are of the same type, for instance, $f_{1,2} = 0.15$.
(2) one layer is cooperative (i.e., $f_1 = 0.0$) and other is competitive (i.e., $f_2 = 1.0$).

Figure 1 illustrates the numerically and analytically calculated amplitudes of the global order parameters R_1 and R_2 for the two configurations of the networks. In Fig. 1(a), both layers have an identical fraction of competitive units ($f_{1,2} = 0.15$), resulting in similar synchronization dynamics in the two layers, highlighting the hysteretic nature of the synchronization transitions. In Fig. 1(b), the first layer is purely cooperative ($f_1 = 0.0$), while the second layer is entirely competitive ($f_2 = 1.0$), leading to distinct behaviors in synchronization. Here, R_1 shows a second-order continuous phase transition while R_2 depicts an abrupt phase transition to the synchronization state at a critical coupling strength, but when the coupling strength crosses the critical value, R_2 continuously goes back to zero value, which means to the incoherent state. Red and blue arrows denote the forward and backward transitions for R_1 and R_2, respectively. Solid red and hollow blue circles represent the analytically derived R_1 and R_2 values, respectively, from Eq. (11). This figure shows an excellent agreement between numerical results and analytical predictions. Each layer consists of $N = 10^3$ nodes connected via random networks with identical average degree $\langle K_{1,2} \rangle = 20$.

Next, we extend the result to a trilayer multiplex network to explore the synchronization dynamics in a more complex situation, and like the previous bilayer model, we take two configurations, namely,

(1) coexistence of competitive and cooperative nodes in both layers, and each pair of replica nodes are of same type, for instance, $f_{1,2,3} = 0.15$.
(2) Two cooperative layers (i.e., $f_{1,2} = 0.0$) and one competitive layer ($f_3 = 1.0$).

Figure 2 presents the variation of the three global order parameters R_1, R_2, and R_3 in two distinct scenarios (as stated above) by changing the coupling strength λ. In Fig. 2(a), all three layers share the same fraction of competitive units ($f_{1,2,3} = 0.15$), leading to similar synchronization transitions across all layers. In Fig. 2(b), the first two layers are fully cooperative ($f_{1,2} = 0.0$), while the third layer is entirely competitive ($f_3 = 1.0$). The forward and backward transitions for R_1, R_2, and R_3 are represented by red, blue, and green arrows, respectively. The analytically calculated values are denoted

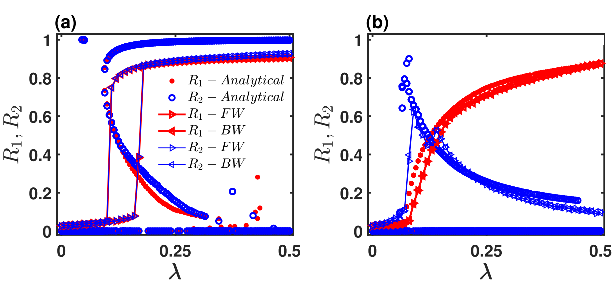

FIG. 1. Variation of the amplitudes of the global order parameters (R_1 and R_2) by changing the coupling strength λ for a bilayer multiplex network under two distinct configurations: (a) both layers have identical fractions of competitive units ($f_{1,2} = 0.15$), and (b) one layer is purely cooperative ($f_1 = 0.0$) while the other is entirely competitive ($f_2 = 1.0$). Red and blue arrows represent forward and backward transitions for R_1 and R_2, respectively, while solid and hollow circles indicate analytically derived values based on Eq. (11) for $L = 2$. Each layer comprises $N = 10^3$ nodes connected via random networks with average degrees $\langle K_{1,2} \rangle = 20$.

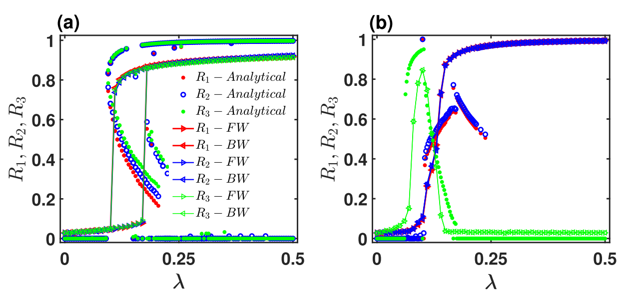

FIG. 2. Numerically and analytically calculated amplitudes of the global order parameters (R_1, R_2, and R_3) for the trilayer multiplex network under two configurations: (a) all layers have identical fractions of competitive units ($f_{1,2,3} = 0.15$), and (b) the first two layers are purely cooperative ($f_{1,2} = 0.0$), while the third layer is entirely competitive ($f_3 = 1.0$). Red, blue, and green arrows represent forward and backward transitions for R_1, R_2, and R_3, respectively. Solid red, hollow blue, and solid green circles are the analytically calculated values of R_1, R_2, and R_3, respectively, based on Eq. (11) for $L = 3$. Here, identical average degree $\langle K_{1,2,3} \rangle = 20$.

by solid red, hollow blue, and solid green circles, again demonstrating excellent consistency with the numerical simulations. Hence, we can say that our analytical predictions derived from the mean-field approach align closely with the numerical simulations on bilayer and trilayer multiplex networks with some configurations depending on the fractional values of the competitive units.

V. EXPLOSIVE SYNCHRONIZATION WITH MIXED TYPES OF INTTERLAYER INTERACTIONS

Now, we will investigate how the mixed type of interactions (i.e., $f_1 \neq f_2 \neq f_3$) influences the explosive synchronization with different average degrees in the layers. In the subsequent sections, we will study in more detail by simulating Eq. (1) and observe the synchronization behaviors in the layers of any bilayer (in Sec. V A) and trilayer (Sec. V B) multiplex networks with different possible configurations. In Sec. V C, we make a comparison of the hysteresis regions by increasing the number of layers of the multiplex networks.

A. Synchronization in bilayer multiplex networks

Figure 3 depicts the explosive synchronization (ES) behavior in a bilayer multiplex network, showing the forward (solid curves) and backward (dotted curves) transitions of the global order parameters R_1 (blue) for layer-1 and R_2 (red) for layer-2. The hysteresis loops, characteristic of ES, exhibit identical critical coupling strengths for both layers during forward and backward transitions, indicating that the synchronization onset is unaffected by the fraction of competitive units.

However, the degree of synchronization, as measured by the height of the order parameters R_1 and R_2, decreases with an increase in the fraction of competitive units. Layer-1, with a lower fraction of competitive nodes ($f_1 = 0.1$), achieves a higher synchronization level compared to layer-2, where the fraction is higher ($f_2 = 0.2$). Both layers consist of $N = 1000$ nodes connected through random intralayer networks with an average degree $\langle K_{1,2}\rangle = 12$.

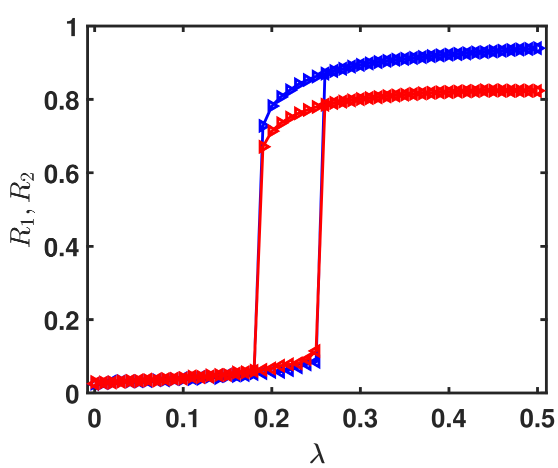

FIG. 3. Explosive synchronization profile of the layers of a bilayer multiplex network. Blue curves are the backward and forward transitions of the order parameter R_1, and the red ones are for R_2. The fraction values of competitive units are $f_1 = 0.1$ and $f_2 = 0.2$. Each layer has $N = 10^3$ total units connected through random networks with average degrees $\langle K_{1,2}\rangle = 12$.

This figure highlights the impact of competitive interactions on synchronization dynamics. While the critical coupling strength remains unchanged, increasing the fraction of competitive units suppresses the degree of synchronization, demonstrating how the balance between competitive and interdependent interactions governs the dynamics of ES in multiplex networks.

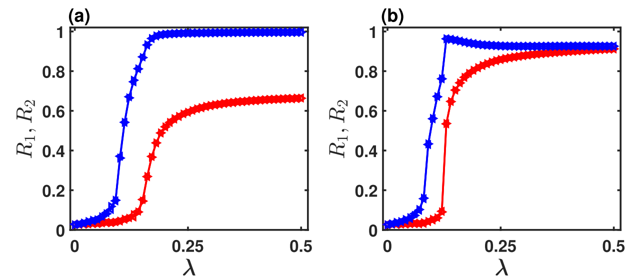

FIG. 4. Phase transition profile of the layers of a bilayer multiplex network. Red curves are the backward and forward transitions of the amplitude of order parameter R_1, and the blue ones are for R_2. (a) The fraction values of competitive units are $f_1 = 0.3$ and $f_2 = 0.1$. Each layer has $N = 10^3$ total units connected through random networks with average degrees $\langle K_1\rangle = 12$ and $\langle K_2\rangle = 42$. (b) The fraction values of competitive units are $f_1 = 0.1$ and $f_2 = 0.2$. Each layer has $N = 10^3$ total units connected through random networks with average degrees $\langle K_1\rangle = 12$ and $\langle K_2\rangle = 42$.

Figure 4 demonstrates the *continuous* phase transition profiles of the global order parameters R_1 (red) for layer-1 and R_2 (blue) for layer-2 in the bilayer multiplex network. Unlike in Fig. 3, where the transition exhibits explosive synchronization with hysteresis, the transitions here are of a continuous type, showing no abrupt jumps or hysteresis. This implies that synchronization occurs smoothly as the coupling strength increases, with both the forward (solid curves) and backward (dashed curves) transitions coinciding, confirming the absence of hysteresis.

In contrast to Fig. 3, where only the fraction of competitive units was varied, in Fig. 4, both the fraction of competitive units and the average degrees of the two layers are varied. In Fig. 4(a), layer-1 has a higher fraction of competitive units ($f_1 = 0.3$) compared to layer-2 ($f_2 = 0.1$), with the average degrees $\langle K_1\rangle = 12$ and $\langle K_2\rangle = 42$. Figure 4(b) presents the reverse configuration, with $f_1 = 0.1, f_2 = 0.2$, and the same average degrees as Fig. 4(a).

The transitions in Fig. 4 reveal that the layer with the higher average degree ($\langle K_2\rangle = 42$) consistently achieves synchronization at a lower critical coupling strength compared to the lower-degree layer ($\langle K_1\rangle = 12$). This highlights how both the fraction of competitive units and the network connectivity contribute to the synchronization dynamics, with higher connectivity promoting easier synchronization and lowering the critical coupling strength required for coherence.

Figure 5 presents the amplitude of the global order parameters R_1 (blue) and R_2 (red) for the bilayer multiplex network, depicting the forward and backward transitions of the order parameters as the coupling strength λ is varied. The figure compares four

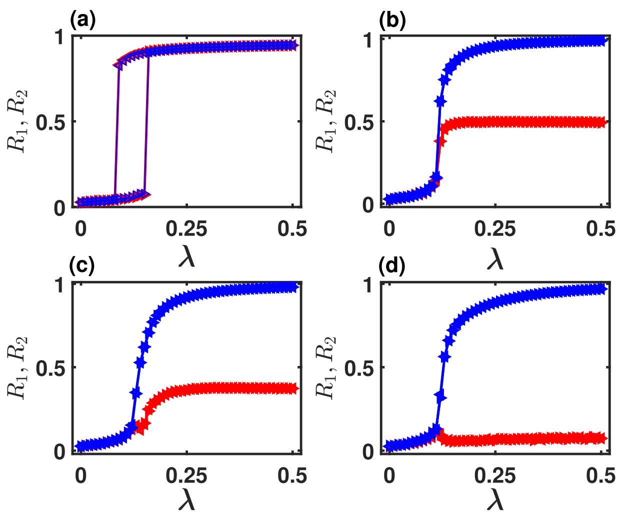

FIG. 5. Amplitude of the global order parameters of the layers of the bilayer multiplex network. Backward and forward transitions of R_1 (*blue*), R_2 (*red*) are plotted with respect to the coupling strength (λ) for different multiplex networks. (a) Both layers have a fraction of competitive units $f_{1,2} = 0.1$, and the average degrees of the layers are taken as $\langle K_{1,2} \rangle = 24$. (b) $f_{1,2} = 0.5$, and $\langle K_{1,2} \rangle = 22$ (c) $f_{1,2} = 0.6$, and $\langle K_{1,2} \rangle = 18$. (d) $f_{1,2} = 0.8$, and $\langle K_{1,2} \rangle = 16$.

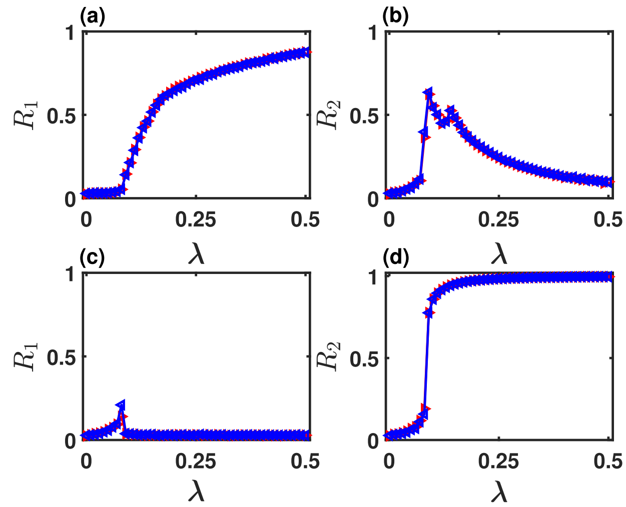

FIG. 6. Amplitude of the global order parameters of the layers of the bilayer multiplex network. Two types of multiplex networks are taken in two panels, and forward and backward R_1, R_2 are plotted by adiabatically increasing and decreasing the coupling strength λ. In the upper panel, (a) all the units of Layer-1 are cooperative ($f_1 = 0.0$), and (b) the units of Layer-2 are all competitive ($f_2 = 1.0$). Both layers are comprised of only competitive units in the lower panel ($f_1 = f_2 = 1.0$). (c) Amplitude of the global order parameter R_1 vs the coupling strength λ, and (d) R_2 vs λ.

different configurations of multiplex networks, varying the fractions of competitive units and the average degrees of the layers.

In panel (a), both layers have the same fraction of competitive units, $f_{1,2} = 0.1$, and the same average degree $\langle K_{1,2} \rangle = 24$. The synchronization is of the first order, as indicated by the presence of hysteresis. Both layers exhibit identical critical coupling values and achieve the same degree of synchronization during the forward and backward transitions.

In Figs. 5(b)–5(d), we observe continuous (second-order) phase transitions without hysteresis. Although the critical coupling values remain the same for both layers in these configurations, the degree of synchronization differs between layers. In Fig. 5(b), with $f_{1,2} = 0.5$ and $\langle K_{1,2} \rangle = 22$, layer-1 reaches a higher synchronization degree ($R_1 = 1$) compared to layer-2, which only synchronizes partially ($R_2 = 0.5$).

Figure 5(c) further reduces the average degree to $\langle K_{1,2} \rangle = 18$, with both layers having $f_{1,2} = 0.6$. In this case, layer-1 again fully synchronizes ($R_1 = 1$), while layer-2 synchronizes to a lower degree ($R_2 = 0.3$), indicating stronger suppression of synchronization due to increased competitive interactions.

In Fig. 5(d), where both layers have the highest fraction of competitive units, $f_{1,2} = 0.8$, and the lowest average degree $\langle K_{1,2} \rangle = 16$, layer-1 reaches its coherent state, but layer-2 remains in its incoherent state. This highlights the extreme impact of competitive interactions and reduced connectivity on synchronization in layer-2, effectively preventing it from reaching coherence.

Figure 6 illustrates two different configurations of a bilayer multiplex network, where the behavior of the global order parameters R_1 (blue) for layer-1 and R_2 (red) for layer-2 are shown as functions of the coupling strength λ. The transitions in this figure are reversible and demonstrate both continuous and explosive synchronization, depending on the configuration of cooperative and competitive units in the layers.

Figures 6(a) and 6(b) refer to the configuration where layer-1 is comprised solely of cooperative units and layer-2 consists of only competitive units. In Fig. 6(a), layer-1 undergoes a continuous phase transition to its synchronized state as the coupling strength increases. The transition is smooth and reversible, indicating second-order synchronization dynamics. In contrast, Fig. 6(b) shows that layer-2, consisting only of competitive units, exhibits a sudden jump to a degree of synchronization around $R_2 = 0.6$ at the critical value $\lambda = 0.07$, followed by a rapid return to the incoherent state as λ decreases. This abrupt change is characteristic of an explosive synchronization transition, but the process remains reversible.

Figures 6(c) and 6(d) refer to the configuration where both layers are comprised entirely of competitive units. In Fig. 6(c), layer-1 remains in an incoherent state throughout the entire range of coupling strength λ, unable to synchronize due to the fully competitive nature of its units. Meanwhile, Fig. 6(d) shows that layer-2 undergoes an explosive phase transition, reaching its coherent state at a critical coupling value $\lambda = 0.07$. The transition is abrupt but reversible, indicating explosive synchronization in layer-2 while layer-1 remains unsynchronized.

Finally, the (λ, f)-parameter space of the bilayer multiplex network is illustrated in Fig. 7, examining the combined effect of coupling strength (λ) and the fraction of competitive units (f_1, f_2) on the synchronization transitions of the two layers. Figures 7(a) and 7(b)

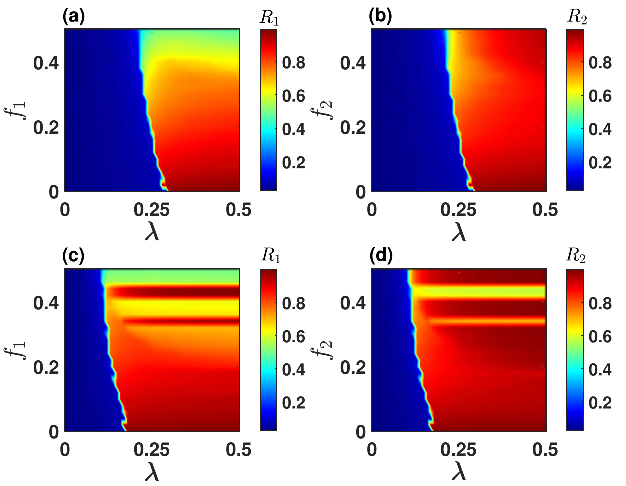

FIG. 7. The (λ, f)-parameter space of the bilayer multiplex network for two configurations, and colorbars represent the forward-phase transition of the amplitudes of the order parameters: (a) and (b) show R_1 and R_2 for $\langle K_{1,2}\rangle = 12$, while (c) and (d) show R_1 and R_2 for $\langle K_{1,2}\rangle = 24$.

depict the forward-phase transitions for the global order parameters R_1 and R_2, respectively, for a network configuration where the average degree of both layers is set to $\langle K_{1,2}\rangle = 12$. Figures 7(c) and 7(d) show similar transitions for the case where the average degrees of the layers are increased to $\langle K_{1,2}\rangle = 24$. In each panel, the colorbars represent the amplitude of the global order parameters across the (λ, f)-space, demonstrating how the synchronization behavior of the layers is influenced by varying competitive interactions and coupling strength. The figures clearly show that as the network connectivity between the units or the fraction value of the competitive units within the layer increases, the critical value of the -phase transition is lowered in both the two layers, and the synchronization region is increasingly enhanced.

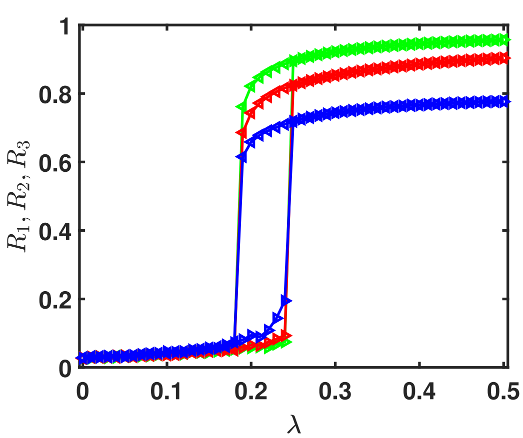

FIG. 8. Amplitudes of the global order parameters of the trilayer multiplex network. The layers' backward- and forward-phase transition concerning the coupling strength (λ) is depicted by three colors: green for R_1, red for R_2, and blue for R_3. Here, the three fractions of the competitive units are taken as $f_1 = 0.05$, $f_2 = 0.15$, $f_3 = 0.25$, and the average degrees of the intralayer random networks are kept fixed at $\langle K_{1,2,3}\rangle = 12$.

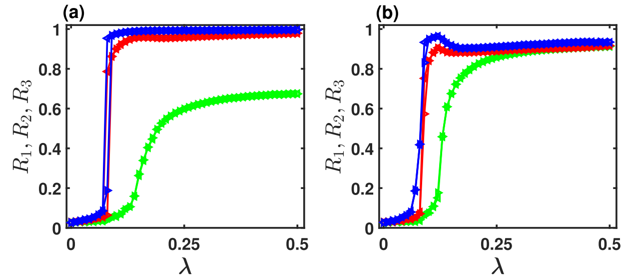

FIG. 9. Phase transition profiles in the trilayer multiplex network. The green, red, and blue curves show the backward and forward transitions of the order parameters R_1, R_2, and R_3, respectively. (a) Fractions of competitive units: $f_1 = 0.3$, $f_2 = 0.2$, $f_3 = 0.1$; average degrees: $\langle K_1\rangle = 12$, $\langle K_2\rangle = 32$, $\langle K_3\rangle = 52$. (b) Fractions of competitive units: $f_1 = 0.1$, $f_2 = 0.2$, $f_3 = 0.3$; average degrees: $\langle K_1\rangle = 12$, $\langle K_2\rangle = 28$, $\langle K_3\rangle = 42$. Each layer has $N = 10^3$ units connected via random networks.

B. Synchronization in trilayer multiplex networks

Moving to the trilayer multiplex network configuration, Fig. 8 presents the amplitude of the global order parameters R_1 (green), R_2 (red), and R_3 (blue) for the trilayer network, showing the forward

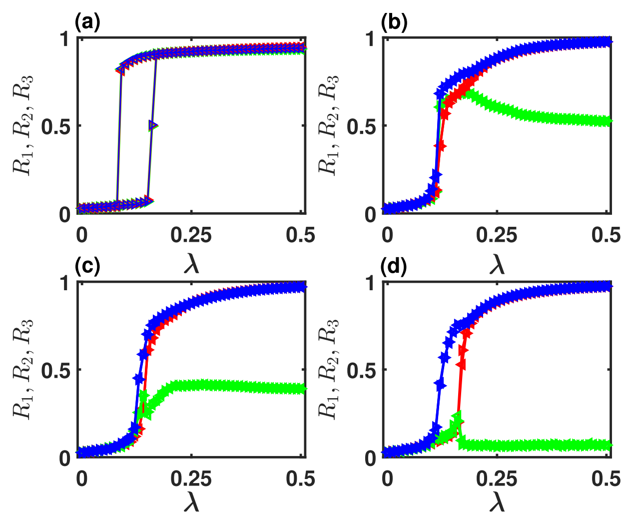

FIG. 10. Amplitude of the global order parameters in the trilayer multiplex network. The backward and forward transitions of R_1 (green), R_2 (red), and R_3 (blue) are plotted against the coupling strength λ for different configurations: (a) $f_{1,2,3} = 0.1$, $\langle K_{1,2,3}\rangle = 24$; (b) $f_{1,2,3} = 0.5$, $\langle K_{1,2,3}\rangle = 22$; (c) $f_{1,2,3} = 0.6$, $\langle K_{1,2,3}\rangle = 18$; (d) $f_{1,2,3} = 0.8$, $\langle K_{1,2,3}\rangle = 16$. Each layer has $N = 10^3$ units connected through random network topology.

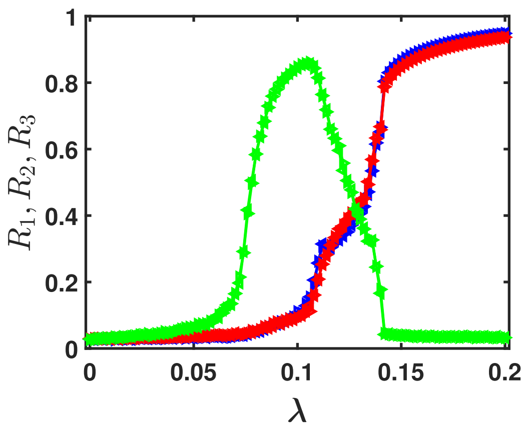

FIG. 11. Amplitude of the global order parameters R_1, R_2, R_3 vs the coupling strength λ. Here, the fraction values of the competitive units for the three layers are taken as $f_1 = 0.0, f_2 = 0.2, f_3 = 1.0$, and all the three intralayer network structures of the multiplex network are random networks of average degree $\langle K_{1,2,3} \rangle = 20$.

and backward transitions as the coupling strength λ is varied. The figure illustrates the synchronization dynamics of each layer with different fractions of competitive units across the layers.

In this configuration, the fractions of competitive units are $f_1 = 0.05, f_2 = 0.15$, and $f_3 = 0.25$, with the average degrees for all layers kept constant at $\langle K_{1,2,3} \rangle = 12$. The transitions in all three layers exhibit typical first-order phase transitions with hysteresis.

Notably, as in the previous case of the bilayered multiplex network configuration (Fig. 3), the degree of synchronization achieved by each layer is inversely related to the fraction of competitive units within the layer. Layer-1, with the smallest fraction of competitive units ($f_1 = 0.05$), reaches the highest level of synchronization, followed by layer-2 with $f_2 = 0.15$, and, finally, layer-3, with the highest fraction of competitive units ($f_3 = 0.25$), achieves the lowest synchronization level. This behavior underscores the suppressive effect of competitive interactions on the synchronization process, as layers with higher fractions of competitive units struggle to achieve full synchronization, even as the coupling strength increases.

Figure 9 illustrates the phase transition behaviors in two configurations of the trilayer multiplex network under varying fractions of competitive nodes and average degrees. Figure 9(a) shows

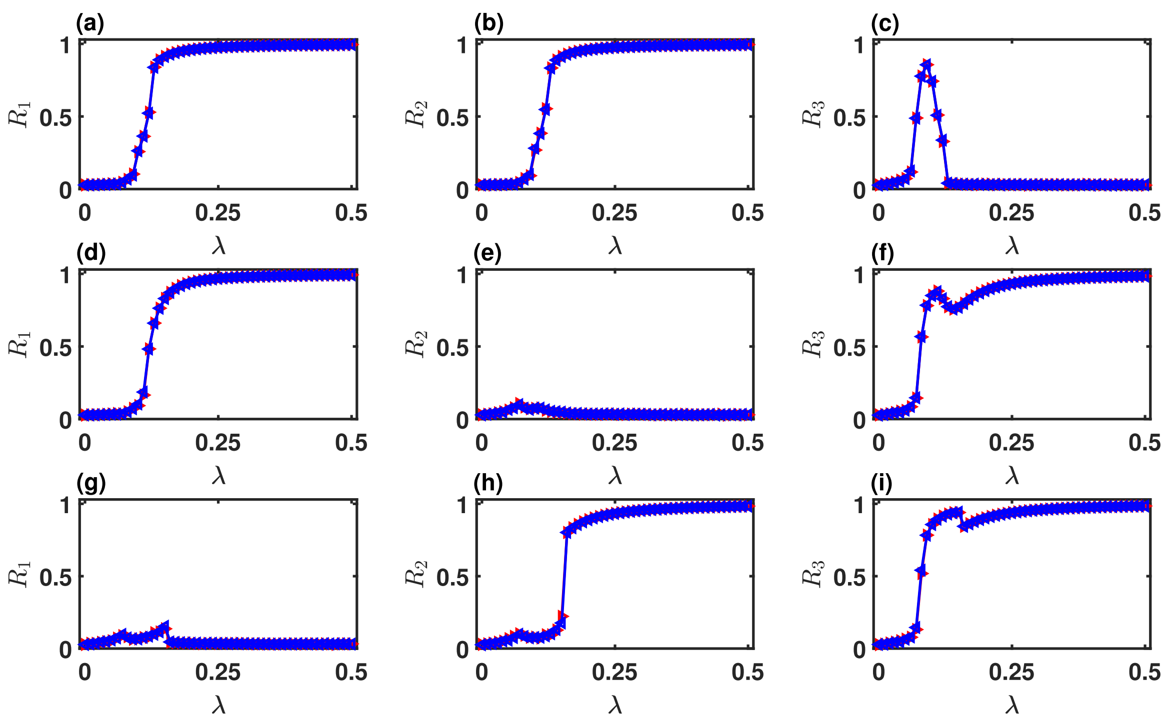

FIG. 12. Evolution of the order parameters of the trilayered multiplex network model vs the coupling strength. Upper panel: two cooperative layers and one competitive layer. (a) and (b): The evolution of the two cooperative layer's order parameters for $f_{1,2} = 0.0$. (c) The order parameter of the competitive layer for $f_3 = 1.0$. Middle panel (d)–(f): One layer is cooperative ($f_1 = 0.0$) and the remaining two are competitive ($f_{2,3} = 1.0$). Bottom panel (g)–(i): Both the three layers are competitive ($f_{1,2,3} = 1.0$).

the phase transition profiles for the fractions of competitive units $f_1 = 0.3$, $f_2 = 0.2$, $f_3 = 0.1$, with average degrees $\langle K_1 \rangle = 12$, $\langle K_2 \rangle = 32$, $\langle K_3 \rangle = 52$. Figure 9(b) illustrates the transitions for $f_1 = 0.1$, $f_2 = 0.2$, $f_3 = 0.3$, and average degrees $\langle K_1 \rangle = 12$, $\langle K_2 \rangle = 28$, $\langle K_3 \rangle = 42$. The forward and backward phase transitions of layer-1, layer-2, and layer-3, i.e., R_1, R_2, and R_3 are represented by green, red, and blue curves, respectively. The results emphasize the role of competitive fractions and average degrees in synchronization dynamics. Higher fractions of competitive units reduce synchronization levels, while layers with higher connectivity achieve synchronization more readily, lowering critical coupling thresholds. However, two layers within the multiplex network exhibit almost identical phase transition profiles in each configuration, while the third layer exhibits distinct behavior, either the synchronization type or the critical value, and the degree of synchronization is different from the other two layers.

Figure 10 illustrates the phase transition behaviors in the trilayer multiplex network for four distinct configurations, varying in the fraction of competitive units (f_1, f_2, and f_3) and the average degrees ($\langle K_1 \rangle$, $\langle K_2 \rangle$, and $\langle K_3 \rangle$) of the layers. In Fig. 10(a), where all layers have identical fractions of competitive units ($f_{1,2,3} = 0.1$) and average degrees ($\langle K_{1,2,3} \rangle = 24$), all three layers exhibit identical first-order phase transitions with hysteresis loops. However, as shown in Figs. 10(b)–10(d), where the fractions of competitive units are increased ($f_{1,2,3} = 0.5$, 0.6, and 0.8, respectively) and the average degrees are progressively reduced ($\langle K_{1,2,3} \rangle = 22$, 18, and 16, respectively), the synchronization dynamics diverge. While two layers exhibit similar phase transitions, the third layer shows a distinct behavior. In particular, as the fraction of competitive units increases, the degree of synchronization for this third layer decreases significantly. In Fig. 10(d), where the fraction of competitive units is highest, the synchronization in this layer is entirely suppressed, with its degree dropping to zero. This demonstrates the critical impact of competitive interactions and reduced connectivity on synchronization dynamics in multiplex networks.

Now, we consider a special configuration of the trilayered multiplex network where layer-1 is comprised of only cooperative units ($f_1 = 0.0$), layer-3 is comprised of only competitive units ($f_3 = 1.0$), and in layer-2, the coexistence of both types of units is present, with the number of competitive units being less than that of cooperative units ($f_2 = 0.2$). The average degrees of the intralayer networks for all three layers are $\langle K_{1,2,3} \rangle = 20$. The phase transitions of layer-1 and layer-2 are almost identical, exhibiting a continuous transition from the incoherent to the coherent state as the coupling strength (λ) increases. However, the phase transition of layer-3 is distinct. It transitions to a coherent state at a critical coupling strength $\lambda = 0.1$, but as λ increases further, it returns to an incoherent state. Each of these transitions is continuous and reversible.

Figure 11 shows the forward and backward transitions of the global order parameters for the three layers in this configuration.

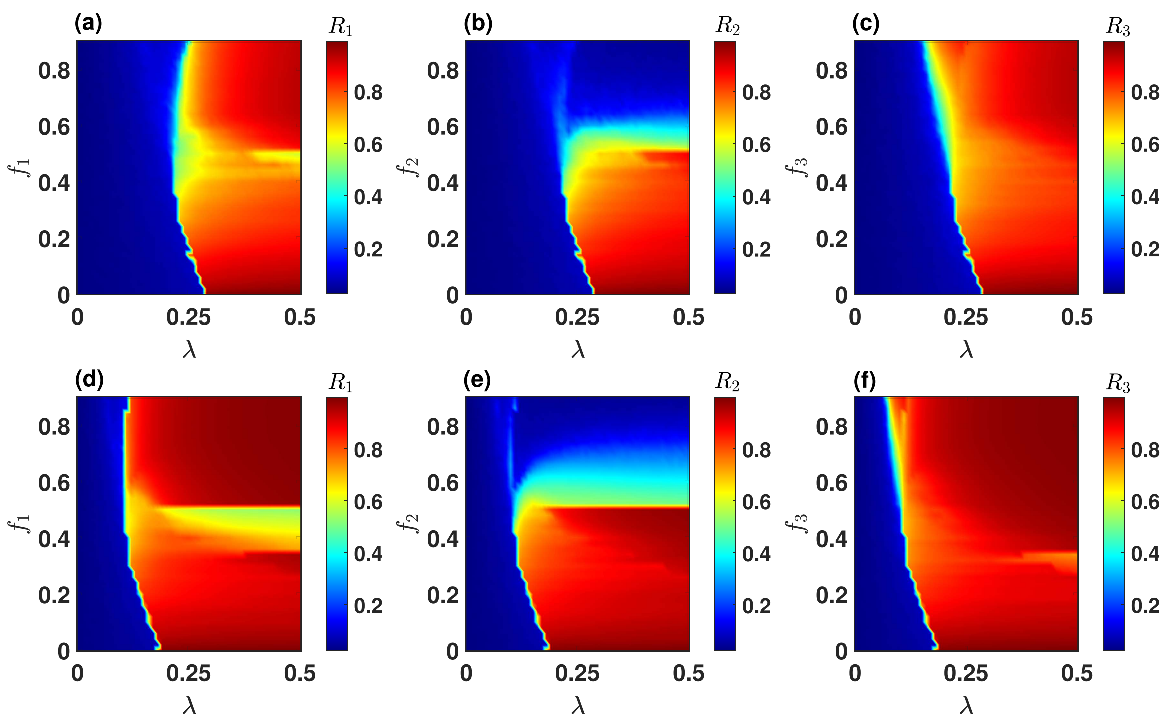

FIG. 13. The (λ, f)-parameter space of the trilayer multiplex network for two configurations, where the colorbars represent the forward-phase transition of the amplitudes of the order parameters. First row panels (a)–(c) depict the order parameters R_1, R_2, and R_3, respectively, for $\langle K_{1,2,3} \rangle = 12$, while the second row panels (d)–(f) show R_1, R_2, and R_3 for $\langle K_{1,2,3} \rangle = 24$.

The transitions (blue and red) of layer-1 and layer-2 reflect typical continuous synchronization dynamics. In contrast, layer-3 exhibits a reentrant behavior (green curve), achieving coherence at a critical coupling strength and subsequently reverting to incoherence. Finally, we consider three configurations for the trilayered multiplex network, where the fraction of competitive units for each layer is either 0 or 1. Figure 12 emphasizes how the number and configuration of competitive layers shape the synchronization dynamics in the trilayered multiplex network. Figures 12(a)–12(c) depict the phase transitions for a multiplex network where only one layer is competitive. In this configuration, the global order parameter of the competitive layer exhibits a continuous and reversible transition in Fig. 12, like R_3 in Fig. 11, as the coupling strength (λ) increases, while the two cooperative layers in Figs. 12(b) and 12(c) show the same second-order phase transition from the incoherent to coherent state. Figures 12(d)–12(f) show the phase transitions for a network where two layers are competitive. Here, the cooperative layers undergo continuous phase transitions to coherence in Fig. 12(d), whereas in Fig. 12(e), one competitive layer always remains in an incoherent state, and the other competitive layer exhibits a second-order phase transition in Fig. 12(f). Figures 12(g)–12(i) present the transitions for the configuration where all three layers are competitive. In this case, also two layers exhibit continuous synchronization transitions as λ increases, but one layer remains in an incoherent state.

Building upon the insights from the previous configurations, Fig. 13 delves deeper into the impact of interlayer dynamics on a more complex trilayer multiplex network. The (λ, f)-parameter space is explored like the previous for the bilayer multiplex network configurations, to understand the combined influence of coupling strength (λ) and the fraction of competitive units (f) on the synchronization transitions across all three layers. Figures 13(a), 13(b), and 13(c) represent the forward-phase transitions of the global order parameters R_1, R_2, and R_3, respectively, for a configuration where all layers have an average degree of $\langle K_{1,2,3}\rangle = 12$. In contrast, Figs. 13(d), 13(e), and 13(f) illustrate the same transitions for a network with increased average degrees $\langle K_{1,2,3}\rangle = 24$. The colorbars depict the amplitude of the global order parameters in each panel, which clearly shows that as the network connectivity between the units increases, the critical value of the forward-phase transition is lowered in the three layers and the synchronization region is increasingly enhanced like the previous case of the bilayer multiplex network. This figure highlights the crucial role that both the fraction of competitive units and the interlayer interaction connectivity play in shaping the synchronization dynamics, offering a comprehensive view of how multiplex network architecture governs the critical thresholds for explosive synchronization. So, in this adaptive framework, for the trilayered multiplex network, we observe that the phase transition profile of one layer can differ significantly from the others by varying the average degrees and the fraction of competitive nodes in the layers. However, when the fraction of competitive nodes is very small and identical across the three layers ($f_{1,2,3} = f$ with $f \ll 1$) and the average degrees are the same ($\langle K_{1,2,3}\rangle = \langle K\rangle$), all three layers exhibit identical first-order phase transitions with hysteresis, having the same critical values and synchronization levels [like Fig. 10(a)]. To understand this, we focus on the phase transition profile of a single layer and compare it with monolayer and bilayer multiplex network configurations, keeping the values of f and $\langle K\rangle$ consistent across all three configurations. This comparison highlights how the interplay of competitive and cooperative interactions influences the synchronization dynamics in multiplex networks with varying numbers of layers, which means configurations and complexities. To further illustrate these effects, we now compare the synchronization behavior across monolayer, bilayer, and trilayer network configurations, examining how increasing structural complexity impacts critical transitions and hysteresis properties.

C. Comparison across monolayer, bilayer, and trilayer networks

Figure 14 illustrates the explosive synchronization profiles for three different network configurations: a monolayer in Fig. 14(a), a bilayered multiplex network in Fig. 14(b), and a trilayered multiplex network in Fig. 14(c). The forward (magenta) and backward (blue) transitions of the global order parameter R_1 are plotted against the coupling strength λ for all configurations, with identical average degrees ($\langle K\rangle = 20$) and fraction values of competitive units ($f = 0.15$) across the layers. It is observed that the critical value of

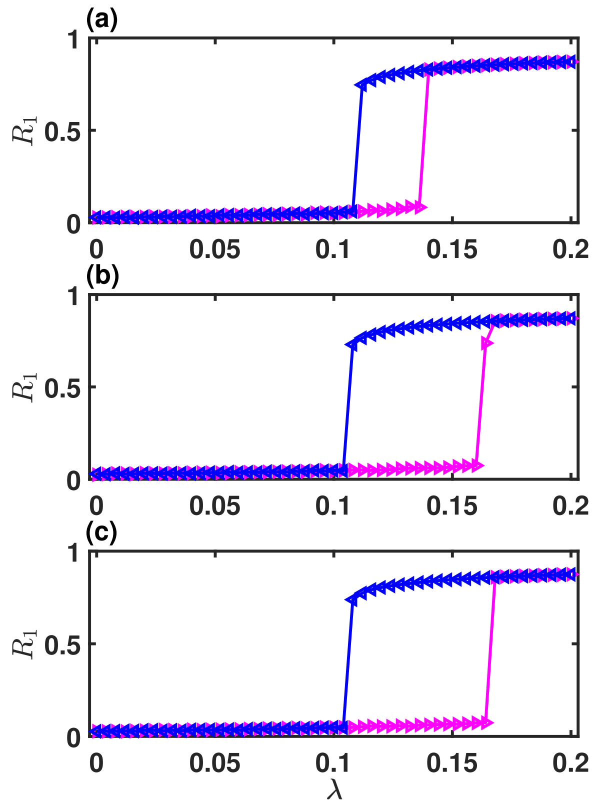

FIG. 14. Explosive synchronization profile for three types of multiplex networks. Forward (magenta) and backward (blue) phase transitions of the order parameters R_1 vs the overall coupling strength λ for (a) a monolayer, (b) a bilayer, and (c) a trilayered multiplex network. The average degrees and the fractional values are fixed at 20 and 0.15, respectively, in every layer of the three types of multiplex networks.

the coupling strength for the first-order forward-phase transition increases as the number of layers in the multiplex configuration rises. Consequently, the hysteresis region also becomes wider with the increase in the number of layers. This indicates that adding more layers in the multiplex structure enhances the system's resilience to synchronization, making the transition to the coherent state more abrupt, requiring a higher coupling strength, and increasing the range of bistability due to competitive and cooperative interlayer dynamics. An increase in hysteresis with the number of layers is often seen as a sign that the synchronized state is becoming more stable since it can resist larger disturbances before losing coherence. However, this can also mean the system is becoming more fragile. If synchronization requires a much higher coupling strength as layers are added, it shows that the system is harder to bring into a synchronized state from the beginning. This makes the dynamics more sensitive to initial conditions and more dependent on the exact value of the coupling. As a result, small changes can lead to sudden, irreversible transitions. So, while the system may appear more stable once synchronized, it is also more prone to failure and harder to control, revealing a hidden fragility behind the increased hysteresis. These results emphasize the significant impact of multiplex architecture on the critical thresholds and hysteresis properties of explosive synchronization.

VI. CONCLUSION

In this study, we proposed a generalized framework for understanding explosive synchronization in adaptive multiplex networks with arbitrary numbers of layers. Our work combines interdependent and competitive interactions simultaneously between the layers through the interlayer connection, offering insights into how these opposing dynamics shape synchronization transitions in complex systems. Through the analytical approach validated by numerical simulations, we demonstrated that the coexistence of competitive and cooperative interactions amplifies hysteretic behavior, particularly when the fractions of the competitive unit in each layer are identical and very small enough ($f_1 = f_2 = f_3 = f \ll 1$), and the width of this loop increases as the number of network layers increases.

The key findings reveal that increasing the fraction of competitive nodes suppresses synchronization and widens the hysteresis loop, while the addition of layers enhances the system's resilience to abrupt synchronization transitions. Furthermore, the adaptive coupling mechanisms we introduced highlight the pivotal role of interlayer coherence in governing synchronization dynamics. Our model generalizes to networks with an arbitrary number of layers, providing scalability and versatility for studying synchronization phenomena across diverse real-world systems, including neural networks, power grids, and social networks.

This work bridges the gap between monolayer and multiplex synchronization models, establishing a robust theoretical foundation for designing and controlling large-scale adaptive systems. Future research can extend the current framework by incorporating more complex interaction mechanisms, particularly within multilayer network structures where diverse coupling strategies coexist. One promising direction is to replace the linear adaptive term with nonlinear adaptive rules, which may capture more realistic and biologically relevant dynamics. Additionally, introducing time delays into the model could provide deeper insights into the temporal aspects of synchronization, especially in systems where interactions are not instantaneous. Together, these extensions would allow for a more comprehensive understanding of synchronization phenomena in complex networked systems.

AUTHOR DECLARATIONS

Conflict of Interest

The authors have no conflicts to disclose.

Author Contributions

Palash Kumar Pal: Conceptualization (equal); Data curation (equal); Formal analysis (equal); Investigation (equal); Methodology (equal); Software (equal); Validation (equal); Writing – original draft (equal). **Nikita Frolov:** Conceptualization (equal); Formal analysis (equal); Investigation (equal); Methodology (equal); Validation (equal); Visualization (equal); Writing – review & editing (equal). **Sarbendu Rakshit:** Conceptualization (equal); Data curation (equal); Formal analysis (equal); Methodology (equal); Software (equal); Visualization (equal); Writing – review & editing (equal). **Alexander E. Hramov:** Conceptualization (equal); Project administration (equal); Supervision (equal); Visualization (equal); Writing – original draft (equal). **Dibakar Ghosh:** Conceptualization (equal); Project administration (equal); Supervision (equal); Visualization (equal); Writing – review & editing (equal).

DATA AVAILABILITY

The data that support the findings of this study are available from the corresponding author upon reasonable request.

APPENDIX: EFFECT OF THE DISTRIBUTIONS OF DEGREE AND FREQUENCY OF NODES ON THE SYNCHRONIZATION PROFILE

Previously, all numerical simulations were carried out using multiplex configurations in which each layer was modeled as a random ER network, with oscillator frequencies $\omega_{l,i}$ drawn from a homogeneous uniform distribution over the interval $[-1, 1]$. To explore the impact of structural and dynamical heterogeneity on the synchronization behavior, we now consider an altered multiplex setup. In this configuration, one of the layers is replaced with a scale-free network that exhibits a heterogeneous degree distribution, and the corresponding oscillator frequencies are sampled from a standard Cauchy distribution, introducing strong dynamical variability due to its heavy-tailed nature. The other layer remains unchanged from the previous models. This arrangement allows us to systematically examine the role of both topological and frequency heterogeneity in shaping the synchronization profile of the system. The phase transition profiles of this multiplex configuration are given in Fig. 15. The forward and backward critical points remain the same for both layers. However, the degree of synchronization gets affected. The layer with a scale-free network topology has lower values of the degree of synchronization. The hysteresis is observed for sufficiently small fractional values of the competitive units in

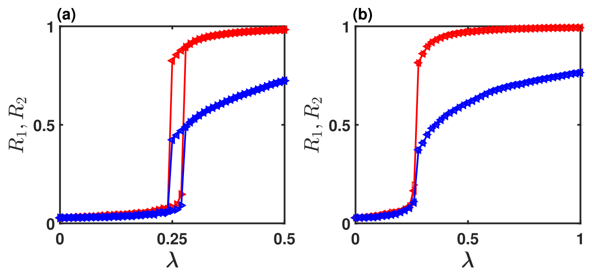

FIG. 15. Amplitudes of the backward and forward global order parameters in the bilayer multiplex network for $N = 10^3$. The phase transition profiles of layers 1 and 2 are represented by the curves in red and blue, respectively. Layer-1 is a random ER network with an average degree $\langle K_1 \rangle = 12$ and having a random homogeneous distribution of frequencies $\omega_{1,i}$ in the range $[-1, 1]$. Layer-2 is a BA network with the average degree $\langle K_1 \rangle = 12$ and the frequencies $\omega_{2,i}$ are drawn from the standard Cauchy distribution. Two fractional values of the competitive units are for two multiplex configurations, viz., (a) $f_{1,2} = 0.01$ and (b) $f_{1,2} = 0.05$.

this multiplex setup [see Fig. 15(a)]. We cannot observe hysteresis even when the fractional values are $f_1 = f_2 = 0.05$ [see Fig. 15(b)]. Whereas in our previous multiplex configuration, when the fractional values were $f_1 = f_2 = 0.15$, we observed a hysteresis region [see Fig. 14(b)].

REFERENCES

[1] A. Pikovsky, M. Rosenblum, and J. Kurths, "Synchronization: A universal concept in nonlinear sciences," (Cambridge University Press, Princeton, 1985).
[2] S. Boccaletti, A. N. Pisarchik, C. I. Del Genio, and A. Amann, *Synchronization: From Coupled Systems to Complex Networks* (Cambridge University Press, 2018).
[3] S. Boccaletti, J. Almendral, S. Guan, I. Leyva, Z. Liu, I. Sendiña-Nadal, Z. Wang, and Y. Zou, "Explosive transitions in complex networks' structure and dynamics: Percolation and synchronization," Phys. Rep. **660**, 1–94 (2016).
[4] D. Pazó, "Thermodynamic limit of the first-order phase transition in the Kuramoto model," Phys. Rev. E **72**, 046211 (2005).
[5] S. V. Buldyrev, R. Parshani, G. Paul, H. E. Stanley, and S. Havlin, "Catastrophic cascade of failures in interdependent networks," Nature **464**, 1025–1028 (2010).
[6] B. M. Adhikari, C. M. Epstein, and M. Dhamala, "Localizing epileptic seizure onsets with Granger causality," Phys. Rev. E **88**, 030701 (2013).
[7] A. Halu, K. Zhao, A. Baronchelli, and G. Bianconi, "Connect and win: The role of social networks in political elections," Europhys. Lett. **102**, 16002 (2013).
[8] B. A. Huberman, R. M. Lukose, and T. Hogg, "An economics approach to hard computational problems," Science **275**, 51–54 (1997).
[9] P. Khanra, P. Kundu, C. Hens, and P. Pal, "Explosive synchronization in phase-frustrated multiplex networks," Phys. Rev. E **98**, 052315 (2018).
[10] A. D. Kachhvah and S. Jalan, "Delay regulated explosive synchronization in multiplex networks," New J. Phys. **21**, 015006 (2019).
[11] S. Jalan, A. D. Kachhvah, and H. Jeong, "Explosive synchronization in multilayer dynamically dissimilar networks," J. Comput. Sci. **46**, 101177 (2020).
[12] A. D. Kachhvah and S. Jalan, "Hebbian plasticity rules abrupt desynchronization in pure simplicial complexes," New J. Phys. **24**, 052002 (2022).
[13] A. D. Kachhvah, X. Dai, S. Boccaletti, and S. Jalan, "Interlayer Hebbian plasticity induces first-order transition in multiplex networks," New J. Phys. **22**, 122001 (2020).
[14] P. S. Skardal and A. Arenas, "Explosive synchronization and multistability in large systems of Kuramoto oscillators with higher-order interactions," in *Higher-Order Systems* (Springer, 2022), pp. 217–232.
[15] M. S. Anwar, N. Frolov, A. E. Hramov, and D. Ghosh, "Self-organized bistability on globally coupled higher-order networks," Phys. Rev. E **109**, 014225 (2024).
[16] X. Zhang, S. Boccaletti, S. Guan, and Z. Liu, "Explosive synchronization in adaptive and multilayer networks," Phys. Rev. Lett. **114**, 038701 (2015).
[17] R. Berner, S. Vock, E. Schöll, and S. Yanchuk, "Desynchronization transitions in adaptive networks," Phys. Rev. Lett. **126**, 028301 (2021).
[18] R. Berner, J. Fialkowski, D. Kasatkin, V. Nekorkin, S. Yanchuk, and E. Schöll, "Hierarchical frequency clusters in adaptive networks of phase oscillators," Chaos **29**, 103134 (2019).
[19] R. Berner, T. Gross, C. Kuehn, J. Kurths, and S. Yanchuk, "Adaptive dynamical networks," Phys. Rep. **1031**, 1–59 (2023).
[20] M. M. Danziger, I. Bonamassa, S. Boccaletti, and S. Havlin, "Dynamic interdependence and competition in multilayer networks," Nat. Phys. **15**, 178–185 (2019).
[21] X. Li, P. K. Pal, Y. Lei, D. Ghosh, and M. Small, "Higher-order interactions induce stepwise explosive phase transitions," Phys. Rev. E **111**, 024303 (2025).
[22] N. Frolov, S. Rakshit, V. Maksimenko, D. Kirsanov, D. Ghosh, and A. Hramov, "Coexistence of interdependence and competition in adaptive multilayer network," Chaos Solitons Fractals **147**, 110955 (2021).
[23] S. Majhi, S. N. Chowdhury, and D. Ghosh, "Perspective on attractive-repulsive interactions in dynamical networks: Progress and future," Europhys. Lett. **132**, 20001 (2020).
[24] S. N. Chowdhury, S. Rakshit, J. M. Buldu, D. Ghosh, and C. Hens, "Antiphase synchronization in multiplex networks with attractive and repulsive interactions," Phys. Rev. E **103**, 032310 (2021).
[25] S. N. Chowdhury, D. Ghosh, and C. Hens, "Effect of repulsive links on frustration in attractively coupled networks," Phys. Rev. E **101**, 022310 (2020).
[26] K. Z. Coyte, J. Schluter, and K. R. Foster, "The ecology of the microbiome: Networks, competition, and stability," Science **350**, 663–666 (2015).
[27] S. N. Chowdhury, J. Banerjee, M. Perc, and D. Ghosh, "Eco-evolutionary cyclic dominance among predators, prey, and parasites," J. Theor. Biol. **564**, 111446 (2023).
[28] S. Roy, S. Nag Chowdhury, P. C. Mali, M. Perc, and D. Ghosh, "Eco-evolutionary dynamics of multigames with mutations," PLoS One **17**, e0272719 (2022).
[29] B. K. Bera, S. Rakshit, D. Ghosh, and J. Kurths, "Spike chimera states and firing regularities in neuronal hypernetworks," Chaos **29**, 053115 (2019).
[30] S. Rakshit, B. K. Bera, E. M. Bollt, and D. Ghosh, "Intralayer synchronization in evolving multiplex hypernetworks: Analytical approach," SIAM J. Appl. Dyn. Syst. **19**, 918–963 (2020).
[31] I.-W. Lee, R. C. Feiock, and Y. Lee, "Competitors and cooperators: A micro-level analysis of regional economic development collaboration networks," Public Adm. Rev. **72**, 253–262 (2012).
[32] H. Daido, "Population dynamics of randomly interacting self-oscillators. I: Tractable models without frustration," Prog. Theor. Phys. **77**, 622–634 (1987).
[33] S. Dixit and M. D. Shrimali, "Static and dynamic attractive–repulsive interactions in two coupled nonlinear oscillators," Chaos **30**, 033114 (2020).
[34] S. Jalan, V. Rathore, A. D. Kachhvah, and A. Yadav, "Inhibition-induced explosive synchronization in multiplex networks," Phys. Rev. E **99**, 062305 (2019).
[35] L. Xie, F. Xiao, and B. Wei, "Explosive synchronization in multilayer networks with inter-layer competition and cooperation," in *2022 41st Chinese Control Conference (CCC)* (IEEE, 2022), pp. 4881–4885.